*European Journal of Soil Science,* March 2001, **52,** 13–24

# Non-equilibrium water flow characterized by means of upward infiltration experiments

J. ŠIMŮNEK[a], O. WENDROTH[b], N. WYPLER[b] & M. T. VAN GENUCHTEN[a]
[a]*George E. Brown Jr Salinity Laboratory, USDA-ARS, Riverside, CA 92507, USA, and* [b]*Institute for Soil Landscape Research, ZALF, 15374 Müncheberg, Germany*

**Summary**

Upward infiltration experiments under tension were used to demonstrate the presence of non-equilibrium flow in soils, the phenomenon that has important implications for the accelerated movement of fertilizers, pesticides, non-aqueous liquids, and other pollutants. Data obtained from these experiments were analysed using the single-porosity Richards equation, as well as a variably saturated, dual-porosity model and a dual-permeability model for characterizing non-equilibrium water flow. The laboratory experiments were carried out on 0.10-m-long soil cores having an internal diameter of 0.10 m. Constant pressure heads of –0.10 and –0.01 m were used as the lower boundary condition. Each infiltration was followed by a single-rate evaporation experiment to re-establish initial conditions, and to obtain the drying soil hydraulic properties. Pressure heads inside the cores were measured using five tensiometers, while evaporative water loss from the top was determined by weighing the soil samples. The data were analysed to estimate parameters using a technique that combined a numerical solution of the governing flow equation (as implemented in a modified version of the Hydrus-1D software) with a Marquardt–Levenberg optimization. The objective function for the parameter estimation was defined in terms of pressure head readings, the cumulative infiltration rate, and the final total water volume in the core during upward infiltration. The final total water volume was used, as well as the pressure head readings during the evaporation part. Analysis of flow responses obtained during the infiltration experiment demonstrated significant non-equilibrium flow. This behaviour could be well characterized using a model of physical non-equilibrium that divides the medium into inter- and intra-aggregate pores with first-order transfer of water between the two systems. The analysis also demonstrated the importance of hysteresis.

## Introduction

Local soil heterogeneity often results in the preferential movement of water and chemicals through macropores. Whereas in unsaturated fractured rock water moves preferentially through fractures and fissures and bypasses much of the rock matrix, in aggregated and macroporous soils water moves both through pores between aggregates, decayed root channels, and earthworm burrows and through the soil matrix itself. An important characteristic of preferential flow is that during wetting the moisture front can propagate quickly to significant depths while bypassing a large part of the matrix pore space. Non-equilibrium preferential movement has received much attention by soil scientists since it has important implications in terms of the accelerated movement of fertilizers, pesticides, non-aqueous liquids, and other pollutants applied to the soil's surface. Water and solutes move to far greater depths, and much faster, than would be predicted using the Richards equation based on area-averaged moisture contents and pressure heads (Beven, 1991).

Preferential flow in structured media is usually described using dual-porosity or dual-permeability models (Pruess & Wang, 1987; Gerke & van Genuchten, 1993; Jarvis, 1999). In both the porous medium is assumed to consist of two overlapping interacting regions, one associated with the inter-aggregate, macropore, or fracture system, and the other with less permeable micropores inside soil aggregates (intra-aggregates), or the rock matrix. While in dual-porosity models the water in the matrix is stagnant, dual-permeability models allow for water to flow in the matrix as well. Models of this type have long been applied to solute transport studies. Especially popular have been dual-porosity models in which distinct mobile and immobile liquid flow regions are assumed (e.g. van Genuchten & Wierenga, 1976), although dual-permeability models in which water can move in both the inter- and intra-aggregate pores are also becoming more

Correspondence: J. Šimůnek. E-mail: jsimunek@ussl.ars.usda.gov
Received 17 April 2000; revised version accepted 8 September 2000

popular (Pruess & Wang, 1987; Gerke & van Genuchten, 1993).

The main disadvantage of dual-porosity or dual-permeability models is that, contrary to models based on a single pore region, they require many more input parameters to characterize both pore systems. Little guidance is available as to how to obtain these parameters, either by direct measurement, *a priori* estimation, or some calibration technique (Beven, 1991; Clothier *et al*., 1995; Jaynes *et al*., 1995). Hence, we need to design experiments or devices that provide (either by inverse modelling or directly) parameters for these relatively complex models. Solute transport parameters of dual-porosity models are often obtained from column experiments on the assumption that water flow is steady (Nkedi-Kizza *et al*., 1984), with codes for parameter estimation such as CXTFIT (Toride *et al*., 1995) and/or STANMOD (Šimůnek *et al*., 1999b) that fit analytical solutions of the transport equation to experimental breakthrough curves. More sophisticated experiments and models are needed also to characterize parameters when flow is unsteady and the soil is unsaturated. These parameters cannot usually be obtained by direct measurement or independent calibration.

Methods for optimizing parameters are well established for estimating hydraulic properties of single-porosity systems (Kool *et al*., 1987). They make it possible to estimate simultaneously the retention and hydraulic conductivity functions from data on transient flow (Kool *et al*., 1987). While they may be applied in many scenarios, numerical inversion of the Richards equation has thus far been limited mostly to one-dimensional experiments in the laboratory (Kool *et al*., 1985; Russo *et al*., 1991; Hudson *et al*., 1996), usually by means of one-step (Kool *et al*., 1985) or multistep (van Dam *et al*., 1994) outflow experiments, but increasingly also using evaporation experiments (Santini *et al*., 1995; Šimůnek *et al*., 1998b).

Experiments on outflow and evaporation both represent desorption and thus lead to parameters associated with drying branches of the soil's hydraulic functions. Often non-equilibrium flow is associated with wetting and not drying, which means that experiments designed to study non-equilibrium flow should involve infiltration. Several applications of inverse analyses to infiltration have been reported, including a hypothetical one-dimensional ponded infiltration experiment (Russo *et al*., 1991), axi-symmetrical infiltration from a tension disc permeameter (Šimůnek *et al*., 1999c), and infiltration from a modified cone permeameter (Gribb *et al*., 1998; Šimůnek *et al*., 1999a). Of these, only Šimůnek *et al*. (1999c), in their experiment on infiltration from a tension disc, observed significant non-equilibrium flow.

Hudson *et al*. (1996) suggested an upward infiltration experiment for laboratory conditions. They imposed a constant flux of water at the bottom of the soil sample, and measured pressure heads inside the sample using tensiometers. To maximize information for the inverse analysis, we suggest here to initiate infiltration by a certain tension at the bottom of the sample, rather than by imposing a boundary flux. Since for flux infiltration the precise amount of water in the sample is always known, the only information characterizing the soil's hydraulic properties is the shape of the wetting front as measured with tensiometers. For tension infiltration, the soil also controls the total amount of water being taken up, thus providing additional information and control for the numerical inversion. We believe that the way water flow responds during transient infiltration can be used to calibrate models for aggregated soils. However, the question remains as to whether such data are enough to identify fairly complex models of flow required to describe the non-equilibrium flow.

The objective of this study was to identify both the drying and wetting branches of the soil's hydraulic properties from consecutive experiments in which the pressure head controlled upward infiltration and evaporation followed. We also examined the validity or reproducibility of hydraulic properties inversely estimated in this manner by doing the infiltration experiments at the same and different boundary conditions of pressure head, and by several evaporation experiments. In addition, we used an experiment on upward infiltration under tension to demonstrate the presence of non-equilibrium flow in the soil. The data were analysed using both equilibrium and non-equilibrium flow models. Non-equilibrium behaviour was characterized using a model of physical non-equilibrium with two regions that divided the pore system into inter- and intra-aggregate pores with first-order transfer of water between the two pore systems. Both dual-porosity and dual-permeability non-equilibrium models were used to analyse the data.

## Experimental

### *Soil*

Cylindrical undisturbed soil samples (0.10 m high and 0.10 m internal diameter) were taken from the 0.05–0.15 m depth layer of the Ap horizon of a sandy loam field site in Lietzen, Brandenburg, Germany. The soil was under conservation tillage, and had a fairly large dry bulk density, $\rho_b$, of 1.65 g cm$^3$, which corresponds to an air-filled porosity of about 0.377 ($= 1 - \rho_b/2.65$). The soil consisted of 62% sand, 32% silt, and 6% clay. The organic carbon content was 0.75%. The structure of this soil was very compact, typical for sandy soils that are intensively tilled and compacted afterwards by traffic. Although aggregates could not be identified, the soil matrix is heterogeneous with respect to bulk density, as was shown by computer tomography. Apparently, ploughing often breaks compacted zones, thus causing development of a fragmented matrix with locally dense regions that alternate with looser ones (H. Rogasik, personal communication).

**Table 1** Summary of experimental conditions

| Experiment | Duration /days | Average final $\theta$ /$m^3m^{-3}$ | Infiltrated volume /mm |
|---|---|---|---|
| Initial condition | NA | 0.068 | |
| Infiltration I, $h_0 = -0.10$ m | 2.5438 | 0.200 | 13.12 |
| Redistribution I | 2.4153 | 0.199 | |
| Evaporation I | 5.1573 | 0.107 | |
| Redistribution II | 9.9713 | 0.103 | |
| Infiltration II, $h_0 = -0.01$ m | 0.9693 | 0.231 | 12.65 |
| Redistribution III | 1.9077 | 0.229 | |
| Evaporation II | 4.4028 | 0.104 | |
| Redistribution IV | 1.8638 | 0.106 | |
| Infiltration III, $h_0 = -0.01$ m | 0.9743 | 0.256 | 14.83 |

*Infiltration experiments*

Prior to the experiments, five pressure transducer tensiometers were installed at 10, 30, 50, 70, and 90 mm depth in the soil (henceforth denoted as locations 1 to 5). The tensiometers, consisting of ceramic cells with an inner diameter of 6 mm, were inserted horizontally into the soil across a length of 50 mm. Good contact between the soil and tensiometers was ensured by using a paste from a fraction of the soil drilled out of the sample before installation. The reaction time of our tensiometers to a 10% change of pressure head was about 3 s at a pressure $h = -0.1$ m and up to 1 minute for $h = -6.0$ m. The samples during upward infiltration were positioned on a porous membrane that was used as a suction plate. At the intended pressure head, the surface of the membrane was in hydraulic equilibrium with a Mariotte reservoir bottle that was placed on a balance. Before and after the infiltration, the soil samples were weighed to determine total amount of water in the samples at the start and at the end. During the first 30 h of the first upward infiltration, weight losses from the reservoir due to water uptake of the soil sample were recorded every 5 minutes using a video camera. Afterwards, when the weight losses became smaller, they were recorded manually. Tensiometer readings were recorded automatically every 2 s. After each infiltration experiment, the sample was sealed and water was allowed to redistribute before starting the evaporation. Additional water was allowed to infiltrate into the soil sample during the redistribution process for one experiment.

Three upward infiltration experiments (I, II, and III) were made, with lower boundary conditions of $h_0 = -0.10, -0.01$, and –0.01 m, respectively. Each infiltration was followed by an evaporation stage, and subsequently by a period of equilibration of the soil sample to re-establish similar initial conditions. Weights of the reservoir bottle during infiltration experiments II and III were recorded with a data logger every 30 s. The larger intervals for weighting the reservoir bottle during infiltration, as compared with measuring pressure heads, was based on the assumption that weights represent a cumulative quality that change much more smoothly than pressure heads, which reflect the movement of moisture fronts. Measuring the pressure heads at longer intervals could quickly lead to missing information about advancing moisture fronts in the sample, but this is less probable when measuring sample weights.

*Evaporation experiments*

Evaporation experiments similar to those by Wendroth *et al*. (1993) and Šimůnek *et al*. (1998b) were done using the same soil column as for the upward infiltration experiments. One modification from the earlier experiments was that evaporation was allowed to proceed slowly, as dictated by the laboratory conditions. The sample was weighed before and after the experiments. During evaporation, tensiometers were recorded automatically every 5 minutes, and the sample weighed every 4 h, except for two intervals during the night.

Prior to each evaporation experiment, after each infiltration, when pressure head changes ceased, hydraulic equilibrium was assumed, and deviations in pressure head from equilibrium were corrected in the calibration functions of the pressure transducers of the five tensiometers by the method of Wendroth *et al*. (1993). Moreover, the calibration of the pressure transducer was divided for each specific transducer into two segments, one between 0 and 1.50 m pressure head, and the other between 1.50 and 6.50 m pressure.

Table 1 summarizes the experimental conditions, including duration of particular parts of each experiment, average water contents in the sample at the beginning and end of each experiment, and the infiltrated volumes. The first infiltration experiment with a supply pressure of –0.10 m lasted 2.5 days. The second and third experiments with applied heads of –0.01 m lasted about 1 day. Evaporation experiments I and II lasted about 5.1 and 4.4 days, respectively. Again, infiltration and evaporation experiments were separated by equilibration periods of between 2 and 10 days. During these both the bottom and the top of the sample were sealed to prevent water loss, thereby allowing water to redistribute inside the sample.

## Methods

Below we give the governing equations for three models describing unsaturated water flow in soils. We first discuss the equilibrium flow of water using the standard single-porosity model, after which we give the governing equations for the models of dual-porosity and dual-permeability non-equilibrium flow. Models of dual-porosity and dual-permeability require many more input parameters than ones of single-porosity. For example, dual-porosity models may require retention parameters for both the mobile and immobile regions, hydraulic conductivity parameters for the mobile region, and parameters of mass transfer between regions. Dual-permeability models require even more parameters since they

must also account for flow in the matrix. They need two functions for water retention, one for the matrix and one for the pores between the aggregates. Also two or three hydraulic conductivity functions are required: one for the inter-aggregate pores, another for the matrix, and sometimes yet another for the interface between the aggregates and the matrix (Gerke & van Genuchten, 1993). We discuss below several options that could minimize the number of parameters needed to describe particular non-equilibrium models.

*Equilibrium flow model*

Water flow under equilibrium conditions may be described using a mixed formulation of the Richards equation:

$$\frac{\partial \theta}{\partial t} = \frac{\partial}{\partial x}\left[K(h)\left(\frac{\partial h}{\partial x} + 1\right)\right], \tag{1}$$

where $x$ is the vertical coordinate (L), taken here to be positive upward, $t$ is time (T), $\theta$ is the water content ($L^3L^{-3}$), $h$ is the pressure head (L), and $K$ is the hydraulic conductivity ($LT^{-1}$).

*Soil hydraulic properties*

We describe the soil hydraulic properties using the van Genuchten–Mualem model (van Genuchten, 1980):

$$S_e(h) = \frac{\theta(h) - \theta_r}{\theta_s - \theta_r} = \frac{1}{(1 + |\alpha h|^n)^m} \tag{2}$$

and

$$K(\theta) = K_s S_e^l [1 - (1 - S_e^{1/m})^m]^2, \tag{3}$$

where $S_e$ is effective fluid saturation (dimensionless), $K_s$ is the saturated hydraulic conductivity ($LT^{-1}$), $\theta_r$ and $\theta_s$ denote the residual and saturated water contents ($L^3L^{-3}$), respectively; $l$ is a pore-connectivity parameter (dimensionless), and $\alpha$ ($l^{-1}$), and $n$ and $m$ ($= 1 - 1/n$) are empirical shape parameters. The above hydraulic functions contain six unknown, independent parameters: $\theta_r$, $\theta_s$, $\alpha$, $n$, $l$ and $K_s$.

*Dual-porosity non-equilibrium flow model*

In dual-porosity models the water in the pores within the aggregates does not move vertically; only that in the pores between the aggregates flows vertically. Thus, intra-aggregate pores represent immobile pockets that can exchange, retain and store water, but are not subject to convective vertical flow. The dual-porosity formulation used here is based on a mixed formulation of the Richards equation to describe water flow in the pores between the aggregates:

$$\frac{\partial \theta_m}{\partial t} = \frac{\partial}{\partial x}\left[K(h)\left(\frac{\partial h}{\partial x} + 1\right)\right] - \Gamma_w, \tag{4}$$

where $\theta_m$ is the inter-aggregate water content (dimensionless) and $\Gamma_w$ is the transfer rate for water from the inter- to the intra-aggregate pores ($T^{-1}$). This rate is described using the first-order rate equation

$$\Gamma_w = \frac{\partial \theta_{im}}{\partial t} = \omega[S_e^m - S_e^{im}], \tag{5}$$

where $\theta_{im}$ is the intra-aggregate water content, $\omega$ is a first-order rate coefficient ($T^{-1}$), and $S_e^m$ and $S_e^{im}$ are effective fluid saturations in the inter- and intra-aggregate regions, respectively.

To minimize the number of parameters in the model, and to distinguish our dual-porosity model from the more comprehensive dual-permeability model described below, we assumed that mass transfer between the inter- and intra-aggregate regions is proportional to the difference in their effective water contents, rather than to their pressure heads (Gerke & van Genuchten, 1993). By using Equation (5) we decreased the number of soil hydraulic parameters, since we need not know the retention and hydraulic conductivity functions for the intra-aggregate region explicitly. Thus, the dual-porosity non-equilibrium model contains nine parameters: the same six parameters ($\theta_r$, $\theta_s$, $\alpha$, $n$, $l$ and $K_s$) as for the equilibrium model (but now pertaining to the inter-aggregate region), two additional factors characterizing the intra-aggregate region (i.e. its residual, $\theta_r^{im}$, and saturated, $\theta_s^{im}$, water contents), and the first-order mass transfer coefficient $\omega$. By further assuming that the residual water content of the inter-aggregate region is equal to zero (hence that residual water is present only in the immobile region), we can decrease the number of model parameters further to eight.

*Dual-permeability non-equilibrium flow model*

In the dual-permeability model Richards' equations can be applied to each of the two pore regions (Gerke & van Genuchten, 1993, 1996). The flow equations for the inter- (subscript m) and intra-aggregate (subscript im) pore systems are, respectively,

$$\frac{\partial \theta_m}{\partial t} = \frac{\partial}{\partial z}\left(K_m \frac{\partial h_m}{\partial z} + K_m\right) - \frac{\Gamma_w}{w_m} \tag{6}$$

and

$$\frac{\partial \theta_{im}}{\partial t} = \frac{\partial}{\partial z}\left(K_{im} \frac{\partial h_{im}}{\partial z} + K_{im}\right) + \frac{\Gamma_w}{1 - w_m}, \tag{7}$$

where $w_m$ is equal to the ratio of the inter-aggregate and total water contents, $\theta_m/\theta$, and the rate of exchange of water

between the inter- and intra-aggregate regions, $\Gamma_w$ ($T^{-1}$), is described as

$$\Gamma_w = \alpha_w(h_m - h_{im}), \tag{8}$$

in which $\alpha_w$ is a first-order mass transfer coefficient ($L^{-1}T^{-1}$). Unlike for the dual-porosity model, the mass transfer, $\Gamma$, in Equation (8) is assumed to be proportional to the difference in pressure heads between the two pore regions. This approach requires estimating retention curves for both pore regions. For porous media with well-defined geometries, the first-order mass transfer coefficient, $\alpha_w$, can be defined as follows (Gerke & van Genuchten, 1996):

$$\alpha_w = \frac{\beta}{a^2} K_a \gamma_w, \tag{9}$$

where $\beta$ is a shape factor that depends on the geometry. The value of $\beta$ ranges from 3 for rectangular slabs to 15 for spherical aggregates. In Equation (9), $a$ is the characteristic length of the aggregate (L) (e.g. the radius of a spherical or solid cylindrical aggregate, or half the width of a rectangular aggregate), and $\gamma_w$ (=0.4) is a dimensionless scaling factor. The effective hydraulic conductivity $K_a$ ($LT^{-1}$) of the interface between a fracture and the matrix can be simply evaluated in arithmetic terms of both $h_m$ and $h_{im}$:

$$K_a(h) = 0.5\{K_a(h_m) + K_a(h_{im})\}. \tag{10}$$

The use of Equation (9) implies that the medium contains geometrically well-defined cylindrical, rectangular or other types of macropores or fractures; see, for example, Edwards *et al*. (1979) and van Genuchten & Dalton (1986). While geometrically based models are conceptually attractive, they may be too complicated for routine applications because aggregated soils and rocks usually contain mixtures of aggregates of various sizes and shapes. Hence, rather than using Equation (9) directly, we lump $\beta$, $a$, and $\gamma_w$ into the definition of the effective hydraulic conductivity $K_a$* at the interface to give

$$\alpha_w = K_a^*(h). \tag{11}$$

The above dual-permeability model has, in its full complexity, many parameters. The porous regions between and within the aggregates are each characterized by the same six soil hydraulic parameters as the equilibrium system. Additionally, estimates of the parameters $K_s^a$*, $\alpha_a$, and $n_a$ are needed to characterize the hydraulic conductivity at the interface when using the Mualem–van Genuchten model. A previous assumption (Gerke & van Genuchten, 1993, 1996) is that the relative conductivity functions of the interface and the intra-aggregate region are the same, requiring thus only the coefficient $K_s^a$* to scale the relative conductivity function. If the pore connectivity parameters, $l$, are equal to 0.5 (Mualem, 1976) and, as before, the residual water content of the mobile region is zero, the number of parameters decreases to 10: $\theta_s^m$, $\theta_r^{im}$, $\theta_s^{im}$, $\alpha_m$, $\alpha_{im}$, $n_{im}$, $n_{im}$, $K_s^m$, $K_s^m$ and $K_s^a$*. Alternatively, the two parameters $\theta_s$ and $w_m$ could be used instead of $\theta_s^m$ and $\theta_s^{im}$.

*Initial and boundary conditions*

The lower and upper boundary conditions for an upward infiltration induced by tension are as follows:

$$h = h_0 \qquad x = 0, t > 0$$

and

$$-K(h)\left(\frac{\partial h}{\partial x} + 1\right) = 0 \qquad x = L,\ t > 0, \tag{12}$$

where $h_0$ is the pressure head applied at the bottom of the sample, and $L$ is the height of the sample. The boundary conditions for the evaporation experiment are

$$-K(h)\left(\frac{\partial h}{\partial x} + 1\right) = 0 \qquad x = 0,\ t > 0$$

and

$$-K(h)\left(\frac{\partial h}{\partial x} + 1\right) = q_{evap}(t) \qquad x = L,\ t > 0, \tag{13}$$

where $q_{evap}$ is the evaporation rate, and for the equilibration period between the infiltration and evaporation experiments

$$-K(h)\left(\frac{\partial h}{\partial x} + 1\right) = 0 \qquad x = 0,\ t > 0$$

and

$$-K(h)\left(\frac{\partial h}{\partial x} + 1\right) = 0 \qquad x = L,\ t > 0. \tag{14}$$

The initial condition for all three experimental phases is given in terms of pressure heads, as measured with the tensiometers:

$$h = h_i(x) \qquad x > 0, t = 0. \tag{15}$$

Equations (1), (4), or (6) and (7), subject to initial and boundary conditions specified in Equations (12) to (15), were solved using a modified version of the Hydrus-1D numerical code (Šimůnek *et al*., 1998a). Modifications involved imple-

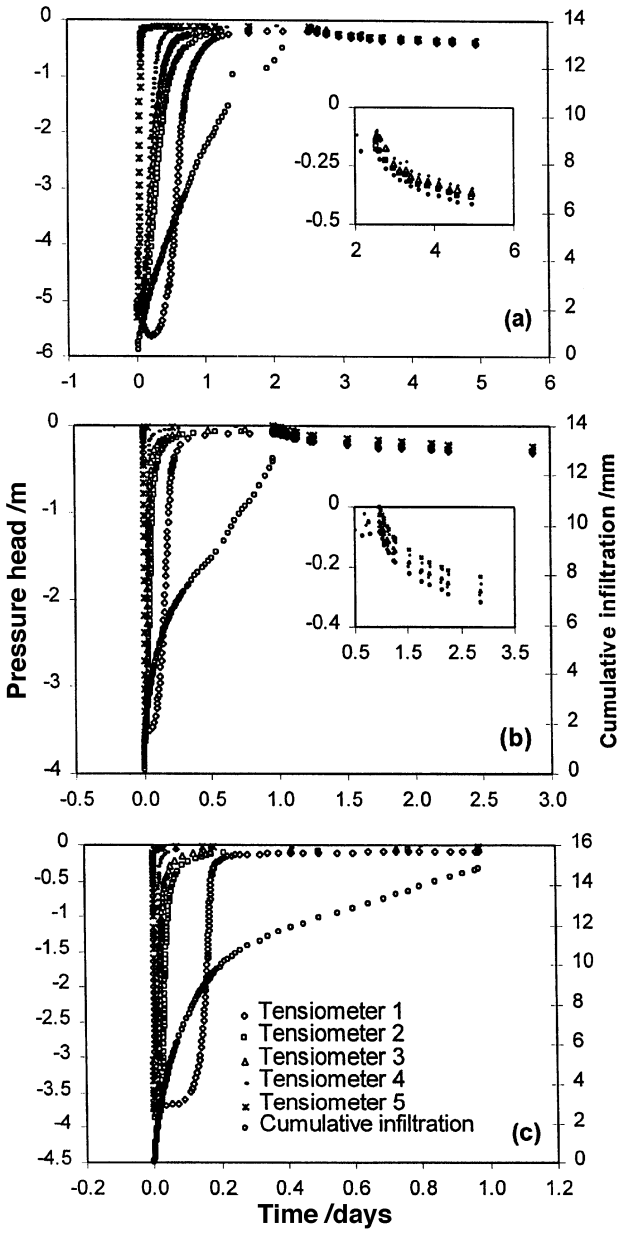


**Figure 1** Measured pressure heads and cumulative infiltration rates for the three infiltration experiments (I, II, and III) subject to applied pressure heads of –0.10 (a), –0.01 (b), and –0.01 (c) m, respectively.

menting the models of dual-porosity and dual-permeability flow.

*Parameter estimation*

We minimized the objective (or merit) function that measures the agreement between measured and modelled data using the Levenberg–Marquardt non-linear method (Marquardt, 1963). The objective function was defined by means of weighted least-squares estimator as follows:

$$\Phi(\beta, q_m) = \sum_{j=1}^{m} \left[ v_j \sum_{i=1}^{n_j} w_{ij} \{ q_j^*(t_i) - q_j(t_i, \beta) \}^2 \right], \qquad (16)$$

where $m$ represents different sets of measurements; $n_j$ is the number of measurements in a particular set, $q_j^*(t_i)$ is the specific measurement at time $t_i$ for the $j$th measurement set, $\beta$ is the vector of optimized parameters (e.g. $\theta_r$, $\theta_s$, $\alpha$, $n$, $K_s$, and $l$ for equilibrium problems, and $\theta_r^{im}$, $\theta_s^{m}$, $\theta_s^{im}$, $\alpha_m$, $\alpha_m$, $n_m$, $n_{im}$, $K_s^{m}$, $K_s^{im}$, and $K_s^{a}$* for non-equilibrium problems), $q_j(t_i,\beta)$ represents the corresponding model predictions for parameter vector $\beta$, and $v_j$ and $w_{ij}$ are weights associated with a particular measurement set $j$ or a measurement $i$ within set $j$, respectively. We assume that the weighting coefficients $w_{ij}$ in Equation (16) are equal to one, that is, the variances of the errors inside a particular measurement set are all the same. The weighting coefficients $v_j$ are given by

$$v_j = \frac{1}{n_j \sigma_j^2}. \qquad (17)$$

This approach views the objective function as the average weighted squared deviation that is normalized by measurement variances $\sigma_j^2$.

## Data analysis

*Analysis of upward infiltration experiments*

Figure 1 shows measured pressure heads and cumulative upward infiltration rates for the three infiltration experiments subject to applied pressure heads of –0.10 (top), –0.01 (middle), and –0.01 (bottom) m. The upper two graphs also present the ensuing redistribution phase of the experiment. Notice that different time scales are used in each figure. The cumulative infiltration curves have a typical shape during the early phase of the infiltration until all five tensiometers register a fairly steady pressure head corresponding to the equilibrium profile. At that moment, according to theory, infiltration should stop, so that the infiltration rate becomes zero. However, we continued monitoring the water intake by the soil sample and noticed a continuing and almost constant infiltration rate in each of the three experiments. The rates stabilized at values of about 2, 8, and 5 mm day$^{-1}$ for experiments I, II, and III, respectively (Figure 2). Tensiometer readings during this second stage of the experiment did not change significantly. Although tensiometers integrate pressure heads along the surface of the tensiometer cup, the readings will have a strong tendency to be close to the largest pressure (closest to zero) in contact with the surface of the tensiometer cup. The continuing infiltration without corresponding changes in the pressure heads suggests that water is redistributing within the soil sample during this second phase of the infiltration. A likely explanation for this redistribution is that water is being

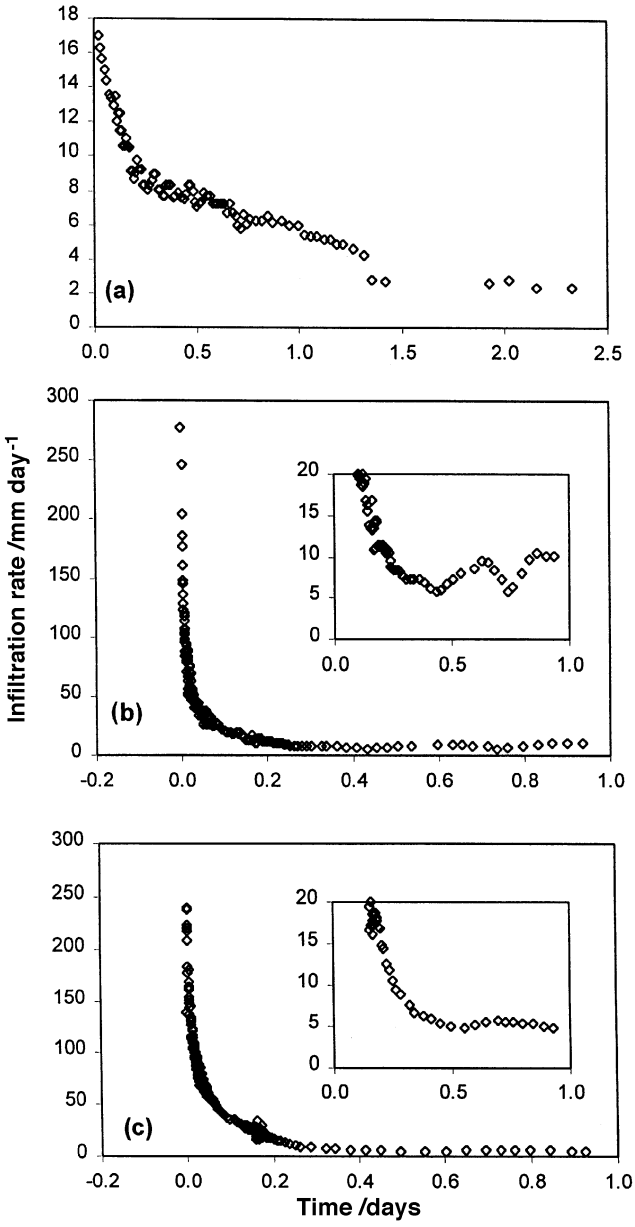


**Figure 2** Measured infiltration rates for the three infiltration experiments (I, II, and III) with applied pressure heads of –0.10 (a), –0.01 (b), and –0.01 (c) cm, respectively.

transferred from the larger (inter-aggregate) to the smaller (intra-aggregate) pores.

The sample was sealed at both sides at the ends of the infiltration experiments, and water was allowed to redistribute within the sample. Since infiltration occurred from the bottom, the final pressure head profile should correspond to the equilibrium state, and no changes, in pressure head readings should be registered afterwards. In our first two experiments, however, the pressure head decreased (suctions increased) in both cases by about 0.22 m throughout the soil sample (Figure 1a,b). The smaller pressure heads and accompanying smaller water contents again suggest slow transfer of water from the inter-aggregate to the intra-aggregate pores.

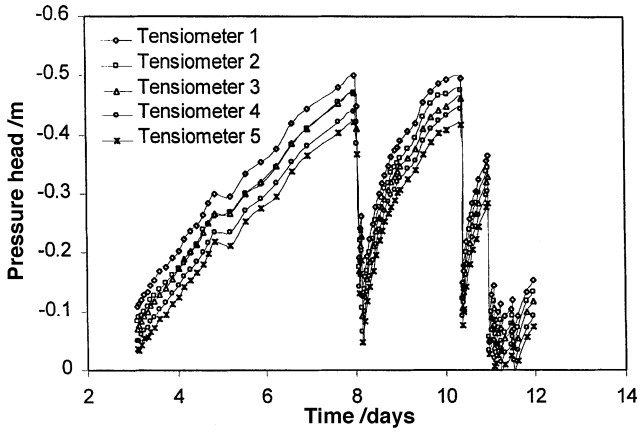


**Figure 3** Measured pressure heads during the redistribution process.

The redistribution of water between the two pore regions was further studied in detail on a second sample that was sealed also at both sides at the end of the infiltration experiment. In this case we allowed water to redistribute within the sample for about 10 days, while small amounts of water were added several times during redistribution to the top of the sample. Figure 3 shows the observed tensiometer readings. Notice that the pressure heads steadily decreased during the first 5 days of redistribution until they reached almost –0.50 m at the top tensiometer. At that time about 0.8 mm of water was added to the top of the sample, which caused the pressure heads to increase almost immediately to about –0.10 m. Similar increases occurred after the other additions of water. We again think that the decrease in pressure is caused by redistribution of water between different pore regions within the soil sample, with the tensiometers registering predominantly pressure heads of the larger and initially wetter pores.

One can estimate the average mobile water content from the advancing moisture front, assuming that there is no transfer of water between the two pore regions. Table 2 presents the average mobile water contents for all three infiltration experiments calculated for each depth where a tensiometer was installed. Since for these calculations we assume that water flows only in the inter-aggregate region, without interaction with the intra-aggregate region, we calculated the average mobile water contents by simply dividing the cumulative infiltration at a time when the centre of the moisture front reached a particular tensiometer by the height of the tensiometer above the bottom of the sample. We assumed that the centre of the water content front corresponded with the value of the pressure head equal to the arithmetic average of the initial and final head. Note from Table 2 that, based on these calculations, only about 6 volume percents participated in the infiltration. This value is between one third and one

**Table 2** Mobile water contents, $\theta_{im}$, calculated from cumulative infiltration and tensiometer readings

| | Experiment | | |
|---|---|---|---|
| Tensiometer /Depth | I | II | III |
| 1 /10 mm | 0.066 | 0.065 | 0.101 |
| 2 /30 mm | 0.052 | 0.050 | 0.060 |
| 3 /50 mm | 0.058 | 0.054 | 0.058 |
| 4 /70 mm | 0.076 | 0.061 | 0.059 |
| 5 /90 mm | 0.066 | 0.042 | 0.038 |
| Average $\theta_{im}$ | 0.0636 | 0.0544 | 0.0632 |
| Overall average $\theta_{im}$ | | 0.0602 | |
| Average final $\theta$ | 0.200 | 0.231 | 0.256 |

fourth of the final water content at the end of the infiltration experiments. Extending this value over the entire sample (height of 0.10 m) shows that only 6 mm of water was needed to 'saturate' the sample fully. This is less than half of the water that actually infiltrated for each infiltration experiment (13.1, 12.7, and 14.8 mm; see Table 1). These numbers clearly indicate that water had to redistribute within the sample from the larger (wetter) inter-aggregate pores (whose pressure heads are measured mostly by the tensiometers) to the smaller intra-aggregate pores within the soil matrix.

The final water contents (Table 1) for all three infiltration experiments were significantly less than the estimated air-filled porosity of 0.377. Significant parts of the intra-aggregate pores must therefore have been left unsaturated at the end of the infiltration experiments, with possibly significant amounts of entrapped air in the intra-aggregate pores. These pores were being gradually filled with water during redistribution (equilibration), a process that must have desaturated the larger pores. It is also generally accepted that the field-saturated (or satiated) water content is much smaller than the porosity because of entrapped and dissolved air. Natural saturation in the laboratory is often only about 0.8–0.9 of the porosity (Klute, 1986), although much smaller values have been reported in the literature.

### *Numerical analysis of upward infiltration assuming equilibrium flow*

First, we optimized the soil hydraulic parameters for all three infiltration experiments using the assumption of equilibrium water flow, i.e. Equation (1). Measured and optimized pressure heads and cumulative infiltrations for the first two upward infiltration experiments with applied pressure heads of –0.10 and –0.01 m are presented in Figure 4. The third infiltration experiment produced very similar results. Optimized parameters for the three infiltration experiments are given in Table 3.

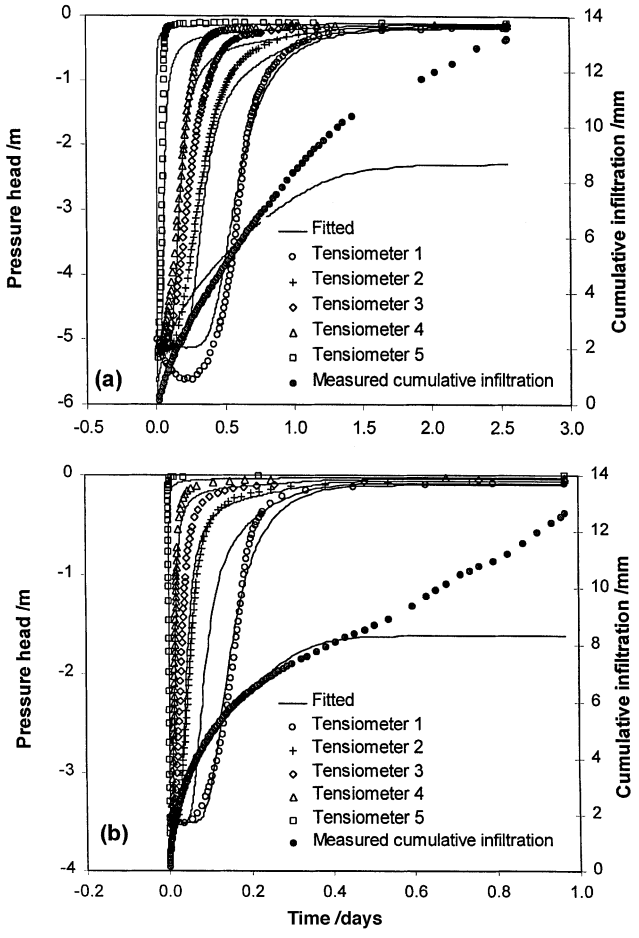


**Figure 4** Measured (symbols) and optimized (lines) pressure heads and cumulative infiltration rates for the first (a) and second (b) upward infiltration experiments having applied pressure heads of –0.10 and –0.01 cm, respectively. Optimized values were calculated using the assumption of equilibrium water flow.

Reasonable correspondence was obtained between measured and calculated pressure heads (Figure 4). As was expected in view of the discussions above, the equilibrium model could not reproduce the cumulative infiltration curves after all tensiometers essentially showed equilibrium with the bottom boundary condition (pressure heads of either –0.10 or –0.01 m). Whereas the measured infiltration rates remained constant for an extended time, the numerical model predicted, as expected, infiltration rates that quickly decreased to zero once the tensiometer readings reached equilibrium. Since this observed behaviour could not be described using the equilibrium model, non-equilibrium models were used as shown below.

### *Numerical analysis of evaporation experiments*

The two evaporation experiments carried out as part of this study were analysed in terms of the equilibrium water flow

**Table 3** Summary of optimization results

| Experiment | Model | $\Phi$ | $\theta_r$ | $\theta_s$ | $\alpha$ /m$^{-1}$ | $n$ | $K_s$ /m day$^{-1}$ | $l$ |
|---|---|---|---|---|---|---|---|---|
| Evaporation I | Equilibrium | 0.00239 | 0.0784 | 0.202 | 1.07 | 2.09 | 0.0332 | 0.0936 |
| Evaporation II | Equilibrium | 0.002731 | 0.0857 | 0.228 | 1.20 | 2.26 | 0.0710 | 0.0753 |
| Infiltration I | Equilibrium | 0.09166 | 0.0045 | 0.211 | 2.82 | 1.24 | 0.0215 | –1.59 |
| Infiltration II | Equilibrium | 0.02824 | 0.0924 | 0.234 | 2.97 | 1.41 | 0.0216 | –2.09 |
| Infiltration III | Equilibrium | 0.02586 | 0.1276 | 0.267 | 2.39 | 1.88 | 0.0165 | –0.0003 |

| Experiment | Model | $\Phi$ | $\theta_r$ | $\theta_s$ | $\alpha$ /m$^{-1}$ | $n$ | $K_s$ /m day$^{-1}$ | $l$ | $w$ | $\omega$ /day$^{-1}$ |
|---|---|---|---|---|---|---|---|---|---|---|
| Infiltration I | Dual-porosity | 0.02903 | 0.00010 | 0.239 | 4.13 | 1.43 | 0.00803 | –1.03 | 0.300 | 0.160 |
| Infiltration II | Dual-porosity | 0.03234 | 0.00018 | 0.306 | 3.94 | 1.37 | 0.0296 | –2.55 | 0.457 | 0.0918 |
| Infiltration III | Dual-porosity | 0.02618 | 0.00337 | 0.416 | 2.60 | 1.61 | 0.0253 | –0.00695 | 0.378 | 0.0616 |

| Experiment | Model | $\Phi$ | $\theta_s$ | $\alpha_{im}$ /m$^{-1}$ | $n_{im}$ | $K_s^{im}$ /m day$^{-1}$ | $\alpha_m$ /m$^{-1}$ | $n_m$ | $K_s^m$ /m day$^{-1}$ | $w$ | $K_s^a$* /m$^{-1}$ day$^{-1}$ |
|---|---|---|---|---|---|---|---|---|---|---|---|
| Infiltration I | Dual-permeability | 0.0549 | 0.283 | 0.629 | 1.46 | 0.149e–7 | 3.09 | 1.63 | 0.0410 | 0.240 | 0.123e–4 |
| Infiltration I | Dual-permeability | 0.0591 | 0.377* | 1.37 | 1.38 | 0.1e–9 | 6.49 | 1.72 | 0.0815 | 0.267 | 0.178e–4 |
| Infiltration II | Dual-permeability | 0.0393 | 0.377* | 0.651 | 1.56 | 0.377e–7 | 9.45 | 1.77 | 0.441 | 0.208 | 0.694e–5 |
| Infiltration III | Dual-permeability | 0.02588 | 0.377* | 0.316 | 1.32 | 0.149e–4 | 3.64 | 1.64 | 0.113 | 0.334 | 0.164e–4 |

*Kept constant during optimization.

model, Equation (1), using the estimation approach suggested by Šimůnek *et al.* (1998b). Measured and optimized pressure heads for both experiments are presented in Figure 5. An excellent correspondence is seen between measured and optimized values. The soil's hydraulic parameters estimated for the two evaporation experiments are also given in Table 3. The two sets of parameters are very similar with the exception of the parameter $\theta_s$, mainly a result of the greater initial water content in the second evaporation experiment. The soil hydraulic functions (both the retention and unsaturated hydraulic conductivity functions) are also almost identical, except for a region close to saturation (Figure 6). This region, however, was beyond the measurement range since both experiments started, because of internal redistribution of water within the sample after the end of the infiltration experiment, with initial pressure heads of about –0.40 m. Nevertheless, Figure 6 shows good consistency and repeatability of results obtained with the two evaporation experiments.

*Numerical analysis of upward infiltration assuming non-equilibrium flow*

All three upward infiltration experiments were next analysed using both models of non-equilibrium water flow. The optimized hydraulic parameters for all inversion runs are given in Table 3. Measured and fitted pressure heads and cumulative infiltration volumes using the dual-permeability model are presented in Figure 7, again only for the first two infiltration experiments. Results with the dual-porosity model were very similar. Calculated pressure heads in Figure 7 correspond reasonably well with the measured values, not only during infiltration, but also during the equilibration or redistribution phase. Notice in particular that the non-equilibrium model accurately described the decrease in the pressure head for all tensiometers during redistribution, when, as we think, water moved from the inter-aggregate to the intra-aggregate pores. The non-equilibrium model also correctly reproduced the continued infiltration when tensiometers already registered constant pressure heads.

For our calculations of non-equilibrium flow we fixed the value of the total water content at saturation equal to the porosity. The fraction of inter-aggregate pores, $w$, was estimated to be between 0.3 and 0.45 when using the dual-porosity model, and between 0.24 and 0.33 when using the dual-permeability model. The values were slightly smaller for the dual-permeability model since the intra-aggregate pores also contribute somewhat to vertical water flow.

Although the confidence in the optimized parameters for the non-equilibrium models is fairly small (because of their large number), the parameters do reflect our conceptual picture of the flow process. For example, the values of $\alpha$ for the intra-aggregate pore system are about one fifth of those for the system of pores between aggregates. Small $\alpha$ values are typical for fine-textured soils. Also, the saturated hydraulic conductivity of the inter-aggregate system was found to be 3 to 7 orders of magnitude larger than $K_s$ for the intra-aggregate

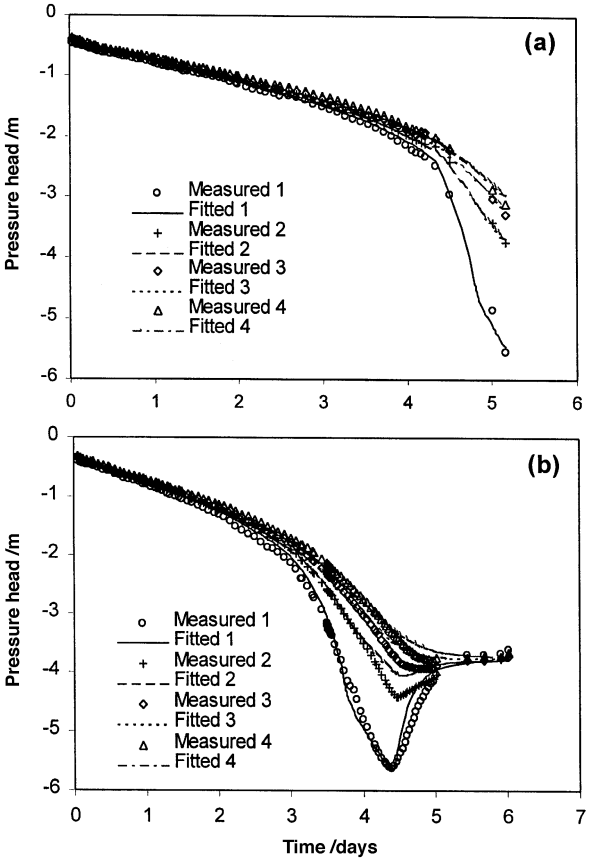


**Figure 5** Measured and optimized pressure heads for the first (a) and second (b) evaporation experiments.

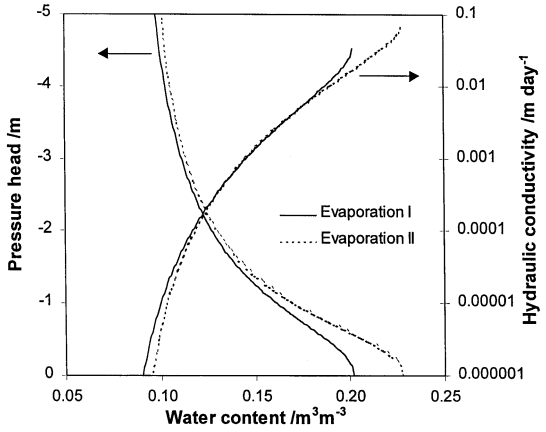


**Figure 6** Soil hydraulic properties obtained by analysing data collected with the evaporation experiments.

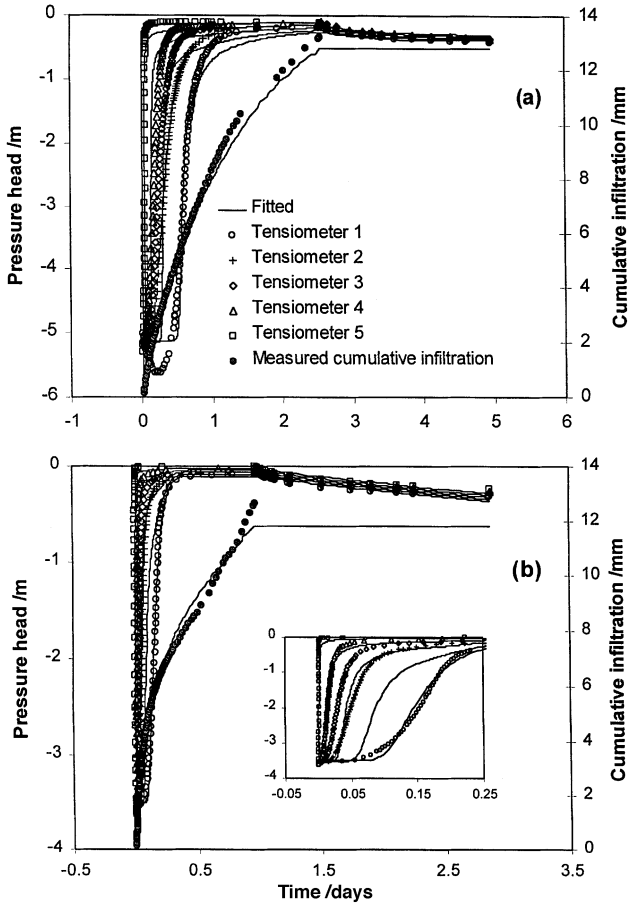


**Figure 7** Measured (symbols) and optimized (lines) pressure heads and cumulative infiltration rates for the first (a) and second (b) upward infiltration experiments having applied pressure heads of –0.10 and –0.01 cm, respectively. Optimized values were calculated using the assumption of non-equilibrium water flow (dual-permeability model).

system and 8 to 10 orders of magnitude larger than $K_s$ for the mass exchange term. Soil hydraulic functions for the inter-aggregate pore region optimized using the dual-permeability model are presented in Figure 8. Notice that the retention and hydraulic conductivity functions have similar shapes, but with larger differences in the estimated values of the saturated water content, $\theta_s^m$, of the inter-aggregate pore region.

## Discussion

The dual-porosity and dual-permeability models require large numbers of quasi-empirical parameters that, in general, must be fitted to experimental data. While both models are likely improvements over existing equilibrium flow models, they remain simplifications of reality with parameters that may be difficult to determine independently. Also, one can hardly expect that complex aggregated pore systems be composed of only two classes of pores, one containing mobile water and one immobile (or less mobile) water. These problems make it difficult to identify parameters in dual-media models by means other than fitting to experimental data.

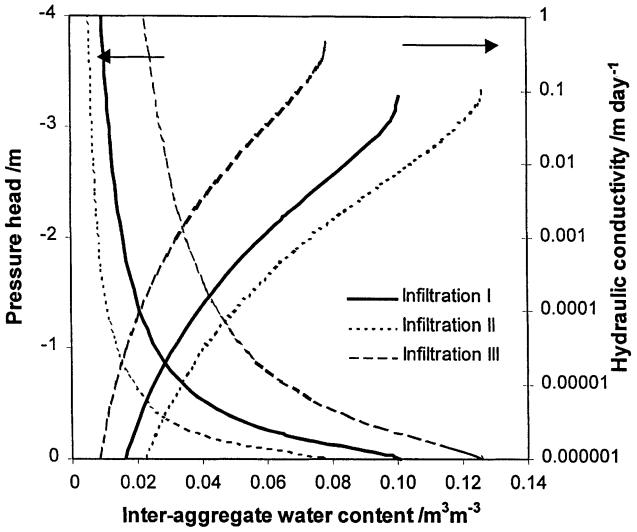


**Figure 8** Soil hydraulic properties of the inter-aggregate pore region obtained by analysing the infiltration/redistribution data using the dual-permeability model.

Many studies have shown that hydraulic parameters of the soil at equilibrium can be obtained by fitting the traditional Richards equation to data on transient water flow. Five ($\theta_r$, $\theta_s$, $\alpha$, $n$, and $K_s$) or even six (plus $l$) soil hydraulic parameters were successfully estimated from, for example, multistep outflow (van Dam *et al*., 1994), evaporation (Šimůnek *et al*., 1998b), and upward infiltration (Hudson *et al*., 1996) experiments. Nevertheless, questions about uniqueness of these optimized parameters still persist. Applying models of dual-porosity or dual-permeability non-equilibrium water flow complicates the inverse problem by invoking additional parameters that make the problem less well-posed, if not ill-posed. Although in our analysis we limited ourselves to eight or nine fitted parameters, the optimization runs always were restarted with different initial guesses of the parameters to ensure as far as possible reaching the global minimum. Table 3 presents parameters for runs having the smallest values of the objective function. Still, we have no complete guarantee that the global minimum of the objective function was obtained in each case.

Hudson *et al*. (1996) used upward infiltration experiments for estimating soil hydraulic parameters, apparently without any problems with non-equilibrium water flow. They carried out their experiments on repacked samples of a loamy fine sand, a soil with a fairly large value of $n$ ($>5$) typical of soil having a narrow pore size distributions. Artificially packed sieved soils generally do not have any identifiable structure. The applied flux at the bottom of the experiment by Hudson *et al*. (1996) was about two orders of magnitude less than the optimized saturated hydraulic conductivity (i.e. the extrapolated value was far beyond the used measurement range). The much slower infiltration used by Hudson *et al*. (1996), and the fact that their soil samples were artificially packed, probably prevented development of non-equilibrium water flow, as was apparent in our experiments.

## Summary and conclusions

Soil's hydraulic properties are often measured in the laboratory using various methods of steady-state or transient drying, such as the pressure plate method, single- or multistep outflow, and evaporation methods. Before such experiments are initiated, samples are typically saturated with the common goal of achieving full saturation (Klute, 1986). Parameters obtained from these measurements are then often used in simulation models to predict water flow near the soil surface. Unfortunately, very little attention is being paid to the fact that the degree of saturation obtained in the laboratory is seldom achieved in the field, and that preferential flow so typical for wetting in the field (Flury *et al*., 1994) can rarely be observed in experiments based on drying. We have suggested above a simple laboratory method that may be able to capture non-equilibrium flow caused by the internal redistribution of water in an aggregated macroporous soil from the inter-aggregate pores to the intra-aggregate pores. The method is based on modification of the upward infiltration experiment (Hudson *et al*., 1996). Infiltration is initiated by a constant or variable tension (close to zero) at the bottom of the soil sample. Water then flows fairly quickly upward through the pores between the aggregates from where it subsequently moves into the aggregates themselves. Fairly fast upward movement of water was observed using tensiometers at several depths.

The dual-porosity and dual-permeability models were successfully used to describe the observed non-equilibrium behaviour. However, our data were too few to optimize a unique set of soil hydraulic parameters needed for calibration of the fairly complex non-equilibrium flow models. Additional measurements or modifications of the upward tension infiltration experiment or both may be needed to obtain supplementary information, especially about the mass transfer process. Initiating the infiltration afresh after an equilibration period could be one possible improvement of the method. Testing the method for soils having different degrees of structural development (from a massive repacked soil to a highly aggregated or macroporous soil) is also desirable.

## References

Beven, K. 1991. Modeling preferential flow: an uncertain future? In: *Preferential Flow* (eds T.J. Gish & A. Shirmohannadi), pp. 1–11. American Society of Agricultural Engineers, St Joseph, MI.

Clothier, B.E., Heng, L., Magesan, G.N. & Vogeler, I. 1995. The measured mobile-water content of an unsaturated soil as a function of hydraulic regime. *Australian Journal of Soil Research*, **33,** 397–414.

Edwards, W.M., van der Ploeg, R.R. & Ehlers, W. 1979. A numerical

study of the effects of noncapillary-sized pores upon infiltration. *Soil Science Society of America Journal*, **43,** 851–856.

Flury, M., Flühler, H., Jury, W.A. & Leuenberger, J. 1994. Susceptibility of soils to preferential flow of water: a field study. *Water Resources Research*, **30,** 1945–1954.

Gerke, H.H. & van Genuchten, M.T. 1993. A dual-porosity model for simulating the preferential movement of water and solutes in structured porous media. *Water Resources Research*, **29,** 305–319.

Gerke, H.H. & van Genuchten, M.T. 1996. Macroscopic representation of structural geometry for simulating water and solute movement in dual-porosity media. *Advances in Water Resources*, **19,** 343–357.

Gribb, M.M., Šimůnek, J. & Leonard, M.F. 1998. Development of a cone penetrometer method to determine soil hydraulic properties. *American Society of Civil Engineers Journal of Geotechnical and Geoenvironmental Engineering*, **124,** 820–829.

Hudson, D.B., Wierenga, P.J. & Hills, R.G. 1996. Unsaturated hydraulic properties from upward flow into soil cores. *Soil Science Society of America Journal*, **60,** 388–396.

Jarvis, N. 1999. Modeling the impact of preferential flow on nonpoint source pollution. In: *Physical Nonequilibrium in Soils: Modeling and Application* (eds H.M. Selim & L. Ma), pp. 195–221. Ann Arbor Press, Chelsea, MI.

Jaynes, D.B., Logsdon, S.D. & Horton, R. 1995. Field method for measuring mobile/immobile water content and solute transfer rate coefficient. *Soil Science Society of America Journal*, **59,** 352–356.

Klute, A. 1986. Water retention: laboratory methods. In: *Methods of Soil Analysis: Part 1*, 2nd edn (ed. A. Klute), pp. 635–662. Agronomy Monograph 9, American Society of Agronomy and Soil Science Society of America, Madison, WI.

Kool, J.B., Parker, J.C. & van Genuchten, M.T. 1985. Determining soil hydraulic properties from one-step outflow experiments by parameter estimation: I. Theory and numerical studies. *Soil Science Society of America Journal*, **49,** 1348–1354.

Kool, J.B., Parker, J.C. & van Genuchten, M.T. 1987. Parameter estimation for unsaturated flow and transport models – a review. *Journal of Hydrology*, **91,** 255–293.

Marquardt, D.W. 1963. An algorithm for least-squares estimation of nonlinear parameters. *SIAM Journal of Applied Mathematics*, **11,** 431–441.

Mualem, Y. 1976. A new model for predicting the hydraulic conductivity of unsaturated porous media. *Water Resources Research*, **12,** 513–522.

Nkedi-Kizza, P., Biggar, J.W., Selim, H.M., van Genuchten, M.T., Wierenga, P.J., Davidson, J.M. & Nielsen, D.R. 1984. On the equivalence of two conceptual models for describing ion exchange during transport through an aggregated oxisol. *Water Resources Research*, **20,** 1123–1130.

Pruess, K. & Wang, J.S.Y. 1987. Numerical modeling of isothermal and non-isothermal flow in unsaturated fractured rock – a review. In: *Flow and Transport through Unsaturated Fractured Rock* (eds D.D. Evans & T.J. Nicholson), pp. 11–22. Geophysics Monograph42, American Geophysical Union, Washington, DC.

Russo, D., Bresler, E., Shani, U. & Parker, J.C. 1991. Analyses of infiltration events in relation to determining soil hydraulic properties by inverse problem methodology. *Water Resources Research*, **27,** 1361–1373.

Santini, A., Romano, N., Ciollaro, G. & Comegna, V. 1995. Evaluation of a laboratory inverse method for determining unsaturated hydraulic properties of a soil under different tillage practices. *Soil Science*, **160,** 340–351.

Šimůnek, J., Šejna, M. & van Genuchten, M.T. 1998a. *The HYDRUS-1D software package for simulating water flow and solute transport in two-dimensional variably saturated media, Version 2.0*. IGWMC-TPS-70, International Ground Water Modeling Center, Colorado School of Mines, Golden, CO.

Šimůnek, J., Wendroth, O. & van Genuchten, M.T. 1998b. A parameter estimation analysis of the evaporation method for determining soil hydraulic properties. *Soil Science Society of America Journal*, **62,** 894–905.

Šimůnek, J., Kodešová, R., Gribb, M.M. & van Genuchten, M.T. 1999a. Estimating hysteresis in the soil water retention function from cone permeameter experiments. *Water Resources Research*, **35,** 1329–1345.

Šimůnek, J., van Genuchten, M.T., Šejna, M., Toride, N. & Leij, F.J. 1999b. *The STANMOD computer software for evaluating solute transport in porous media using analytical solutions of convection-dispersion equation, Versions 1.0 and 2.0*. IGWMC-TPS-71, International Ground Water Modeling Center, Colorado School of Mines, Golden, CO.

Šimůnek, J., Wendroth, O. & van Genuchten, M.T. 1999c. Estimating unsaturated soil hydraulic properties from laboratory tension disc infiltrometer experiments. *Water Resources Research*, **35,** 2965–2979.

Toride, N., Leij, F.J. & van Genuchten, M.T. 1995. *The CXTFIT code for estimating transport parameters from laboratory or field tracer experiments, Version 2.0*. Research Report 137, US Salinity Laboratory, US Department of Agriculture, Agricultural Research Service, Riverside, CA.

Van Dam, J.C., Stricker, J.N.M. & Droogers, P. 1994. Inverse method to determine soil hydraulic functions from multistep outflow experiment. *Soil Science Society of America Proceedings*, **58,** 647–652.

Van Genuchten, M.T. 1980. A closedform equation for predicting the hydraulic conductivity of unsaturated soils. *Soil Science Society of America Journal*, **44,** 892–898.

Van Genuchten, M.T. & Wierenga, P.J. 1976. Mass transfer studies in sorbing porous media, I. Analytical solutions. *Soil Science Society of America Journal*, **40,** 473–481.

Van Genuchten, M.T. & Dalton, F.N. 1986. Models for simulating salt movement in aggregated field soils. *Geoderma*, **38,** 165–183.

Wendroth, O., Ehlers, W., Hopmans, J.W., Kage, H., Halbertsma, J. & Wösten, J.H.M. 1993. Reevaluation of the evaporation method for determining hydraulic functions in unsaturated soils. *Soil Science Society of America Journal*, **57,** 1436–1443.